Nonlinear Vibration Analysis of Metal Foam Nanobeams with Varying Porosity

Layla M. Nassir, Nadhim M. Faleh*, Raad M. Fenjan, Mustafa Qahtan Hadi Al-Ghrari, and Mamoon A. A. Al-Jaafari

Department of Mechanical, College of Engineering, Mustansiriyah University, Baghdad, Iraq
Email: layla_matter@uomustansiriyah.edu.iq (L.M.N.); dr.nadhim@uomustansiriyah.edu.iq (N.M.F.); dr.raad2017@uomustansiriyah.edu.iq (R.M.F.); mostafaqahtan@gmail.com (M.Q.H.A.-G.); dr.mamoonal-jaafare@uomustansiriyah.edu.iq (A.A.A.-J.)
*Corresponding author

***Abstract*—This study concerns the nonlinear vibrations of thick porous nanobeams using nonlocal elasticity to incorporate small-scale effects. Unlike previous studies, which primarily focus on linear vibrations, uniform porosity, or neglect variations in porosity distributions, this work examines the coupled influence of nonlocal effects, geometric nonlinearity, and varying porosity distributions (including symmetric and asymmetric profiles) on the dynamic behaviour of metal foam nanobeams. This is a closed-form solution, thus offering a detailed investigation of the vibrational behaviour of the nanobeam regarding nonlocal effects accompanying the void distribution and physical parameter variations. Such results indicate that porosity distribution and void density make a considerable difference to the natural frequencies and mode shapes of a nanobeam and, hence, have something important to say in the design of lightweight, high-strength nanoscale structures. It identifies, particularly for use in advanced engineering applications, as the study that fills a research gap between linear and nonlinear analyses of porous nanobeams. This study fills a research gap by providing a comprehensive analysis bridging the divide between linear and nonlinear analyses of porous nanobeams and exploring the effects of varying porosity profiles, which were not previously addressed.**

***Keywords*—non-linear vibration, beam theory, metal, nanobeam, elasticity**

I. Introduction

Metal foams are lightweight metallic materials characterized by varying porosity levels. This variation in porosity leads to significant differences in properties compared to conventional metals. For imperfect metals, these porosity variations notably influence the material properties. These variations also impact on the vibration frequencies of the structures made from metal foam. That phenomenon has been explored in the studies conducted [1, 2].

In contrast to metal foams, Functionally Graded (FG) materials, which may include a combination of ceramic and metal components, also exhibit significant effects due to variations in porosity. Research conducted by Mechab *et al.* [3] and Mirjavadi *et al.* [4, 5] emphasizes this importance. Pores can form in the transitional phase between the ceramic and metal components in these materials. To gain a better understanding of the vibrational behavior of engineering structures made from these materials, studies by Wattanasakulpong *et al.* [6], Yahya *et al.* [7], and Atman *et al.* [8, 9] have been conducted. Recent research has focused on nanoscale engineering structures, which involve nanomechanical systems. Though, a significant challenge in these articles is selecting an appropriate elastic theory that considers small-scale effects. The influence of size dependence can be explained using the scale parameter included in the nonlocal elastic theory proposed by Eringen [10]. The term "nonlocal" indicates that the stresses are not confined to local regions, as we discuss stress fields within nanoscale structures. Many researchers [11–38] have recognised these principles and have applied this theory to analyze the mechanical properties of small engineering structures. The current study investigates the geometrically nonlinear vibrational response of thinned, thick, porous nanobeams. For this purpose, the nonlocal elasticity theory is employed to formulate the nanobeam model. The presence of voids or pores influences the material properties of the nanobeam; therefore, their effects, along with variations in void distributions, are considered in this study. The closed-form solution of the nonlinear problem, adopted from previous research, is utilized. Ultimately, this study aims to demonstrate how the nonlocal scale, void distribution, number of voids, and geometric properties affect the nonlinear vibrational characteristics of metal foam nanobeams.

The comparison of this study with previous literature can be summarised as follows: (1) The research conducted by Chen *et al.* [1] and Rezaei and Saidi [2] has focused on uniform porosity distribution in functionally graded beams and plates. These significant contributions detail the dynamics of linear porous structures, yet they do not

Manuscript received December 19, 2024; revised January 20, 2025; accepted March 24, 2025; published July 10, 2025.

account for variations in porosity distributions or void density. Our simulation aims to introduce non-uniform porosity distribution as a foundation for discussing nonlinear vibration phenomena in nanobeams, providing a model that more accurately reflects real material systems. (2) Nonlinear Vibration Analysis: Most existing studies, such as those by Wattanasakulpong and Ungbhakorn [6] and Yahia *et al.* [7], have performed linear vibrational analyses of porous structures. Although these investigations have been informative and have significantly advanced our understanding of the dynamic behavior of porous materials, large amplitudes or thicknesses in the structures render geometrically nonlinear effects quite pronounced. This study addresses that gap by presenting a nonlinear formulation to analyse the vibrational response of thick porous nanobeams, thereby offering a more comprehensive view of their dynamic behavior. (3) Small-scale effects are crucial to understanding the mechanical behavior of nanoscale structures. Most research, such as that by Eringen [10] and Natarajan *et al.* [11], addresses these effects within the framework of nonlocal elasticity theory. However, these studies typically focus on nanobeams vibrating linearly and do not account for the influence of porosity alongside geometric nonlinearity. In the present work, we further apply nonlocal elasticity theory to investigate the nonlinear vibrational behavior of porous nanobeams, demonstrating the significant impact of small-scale effects on their dynamic response. (4) Closed-Form Solutions: Numerical methods, such as finite element analysis, have been widely accepted as viable means to study vibrational behavior in porous structures (e.g., Al-Maliki *et al.* [14]). However, closed-form solutions are preferred due to their computational efficiency and the ease with which physical insight can be obtained. In this study, a closed-form solution of the nonlinear governing equations is adopted, presenting a possibility to discuss in detail the influence of different parameters on the vibrational characteristics of metal foam nanobeams, particularly nonlocal fields, void distribution, and geometric properties. A complete study of thick porous nanobeams' geometrically nonlinear vibrational response is presented, considering the variation in porosity distributions and void density.

Recent research has focused on nanoscale engineering structures involving nanomechanical systems. A significant challenge in these articles is selecting an appropriate elastic theory considering small-scale effects. Ultimately, this study aims to demonstrate how the nonlocal scale, void distribution, number of voids, and geometric properties affect the nonlinear vibrational characteristics of metal foam nanobeams.

Table I highlights that this study addresses a combination of factors not previously explored together, namely the nonlinear vibrational behavior of thick, porous nanobeams with varying porosity profiles under the nonlocal elasticity framework. This comprehensive approach allows for a more realistic representation of nanobeam behavior and significantly advances the field. This study was conducted by utilizing several related papers and researchers [39–48].

TABLE I. THE COMPARISON OF THIS STUDY WITH PREVIOUS LITERATURE CAN BE SUMMARIZED IN

Feature	Chen *et al.* [1], Rezaei and Saidi [2]	Wattanasakulpong and Ungbhakorn [6], Yahia *et al.* [7]	Eringen [10], Natarajan *et al.* [11]	Al-Maliki *et al.* [14]	This Study
Porosity Distribution	Uniform	(Not specified/implied uniform)	(Not considered)	(Can be varied in FEA, but not explicitly addressed)	Varying (Uniform, Non-uniform 1 & 2)
Vibration Analysis	Linear	Linear	Linear	Linear (in the referenced work, though FEA can handle nonlinearity)	Nonlinear
Small-Scale Effects	(Not considered)	(Not considered)	Nonlocal Elasticity	(Not considered in the referenced work)	Nonlocal Elasticity
Solution Method	Analytical	Analytical	Analytical	Finite Element Analysis	Closed-Form Analytical
Nanobeam Geometry	Thin/Classical Beam Theory (implied)	Thin/Classical Beam Theory (implied)	Thin/Classical Beam Theory (in many cases)	(Can be varied in FEA)	

II. THE MODELING

A. Porous Metal Nanobeam

Fig. 1 presents a schematic of the metal foam nanobeam considered in this study. The nanobeam has a length of L and a thickness of h. The x-axis is taken along the longitudinal direction of the nanobeam, with the origin at the left end. The z-axis represents the thickness direction, with $z = 0$ located at the mid-plane of the nanobeam.

The distribution of voids or pores within them influences the material properties of metals. These cavities can be distributed either uniformly or non-uniformly. In cases of non-uniform distribution, we can further classify them as either symmetric (non-uniform type 1) or asymmetric (non-uniform type 2). The expressions for the material properties, such as the elastic modulus (E) and mass density, of metal foams are provided below:

$$E = E_2(1-e_0\mathrm{X}),\ \rho = \rho_2\sqrt{(1-e_0\mathrm{X})} \quad \text{Uniform} \qquad (1)$$
$$\mathrm{X} = \frac{1}{e_0} - \frac{1}{e_0}\left(\frac{2}{\pi}\sqrt{1-e_0} - \frac{2}{\pi} + 1\right)^2$$

$$E(z) = E_2\left(1-e_0\cos\left(\frac{\pi z}{h}\right)\right),\ \rho(z) = \rho_2\left(1-e_m\cos\left(\frac{\pi z}{h}\right)\right) \quad \text{Non uniform 1} \qquad (2)$$

$$E(z)=E_2(1-e_0\cos\left(\frac{\pi z}{2h}+\frac{\pi}{4}\right)),\rho(z)=\rho_2(1-e_m\cos\left(\frac{\pi z}{2h}+\frac{\pi}{4}\right))$$

Non uniform 2 (3)

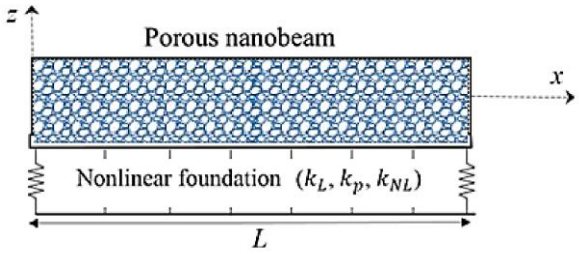

Fig. 1. A metal beam with a stretchable base.

In the definition provided, the exponent 2 indicates the maximum value of the material property. Additionally, two coefficients, e_0 and e_m, are related to pore quantity and mass distribution.

$$e_0=1-\frac{E_2}{E_1}=1-\frac{G_2}{G_1},e_m=1-\sqrt{1-e_0} \quad (4)$$

The nanobeams investigated in this work are categorized as thick. Therefore, it is very important to implement a second-order thick beam perfectly. In this work, we used a refined model by considering the axial and lateral displacements, which are denoted as u_1 and u_3.

$$u_1(x,z,t)=u(x,t)-(z-z^*)\frac{\partial w_b}{\partial x}-[f(z)-z^{**}]\frac{\partial w_s}{\partial x} \quad (5)$$

$$u_3(x,z,t)=w(x,t)=w_b(x,t)+w_s(x,t) \quad (6)$$

where:
$u(x,z,t)$ is the total axial displacement.
$u(x,t)$ is the axial displacement of the mid-plane.
$w_0(x,t)$ is the transverse displacement due to bending.
$w_s(x,t)$ is the transverse displacement due to shear.
$w(x,t)$ is the total transverse displacement.
z is the coordinate along the thickness direction.
z^* is the location of the neutral axis.
z^{**} is a term related to the transverse shear stress distribution.
w is total deflection.

$$f(z)=-\frac{z}{4}+\frac{5z^3}{3h^2} \quad (7)$$

where $f(z)$ is the shape function that defines the distribution of the transverse shear stress/strain through the thickness.

$$z^*=\frac{\int_{-h/2}^{h/2}E(z)\,z\,dz}{\int_{-h/2}^{h/2}E(z)\,dz},\ z^{**}=\frac{\int_{-h/2}^{h/2}E(z)\,f(z)dz}{\int_{-h/2}^{h/2}E(z)\,dz} \quad (8)$$

Due to the offered theory of beam, many researchers have resulting the governing equations in the form described below:

$$\frac{\partial N_x}{\partial x}=I_0\frac{\partial^2 u}{\partial t^2}-I_1\frac{\partial^3 w_b}{\partial x\partial t^2}-I_3\frac{\partial^3 w_s}{\partial x\partial t^2} \quad (9)$$

$$\frac{\partial^2 M_x^b}{\partial x^2}=-\frac{\partial}{\partial x}(N_x\frac{\partial(w_b+w_s)}{\partial x})+k_L(w_b+w_s)-k_P\frac{\partial^2(w_b+w_s)}{\partial x^2}+k_{NL}(w_b+w_s)^3$$
$$+I_0\frac{\partial^2(w_b+w_s)}{\partial t^2}+I_1(\frac{\partial^3 u}{\partial x\partial t^2})-I_2(\frac{\partial^4 w_b}{\partial x^2\partial t^2})-I_4(\frac{\partial^4 w_s}{\partial x^2\partial t^2}) \quad (10)$$

$$\frac{\partial^2 M_x^s}{\partial x^2}+\frac{\partial Q_{xz}}{\partial x}+\frac{\partial}{\partial x}(N_x\frac{\partial(w_b+w_s)}{\partial x})-k_L(w_b+w_s)+k_P\frac{\partial^2(w_b+w_s)}{\partial x^2}$$
$$-k_{NL}(w_b+w_s)^3=I_0\frac{\partial^2(w_b+w_s)}{\partial t^2}+I_3(\frac{\partial^3 u}{\partial x\partial t^2})-I_4(\frac{\partial^4 w_b}{\partial x^2\partial t^2})-I_5(\frac{\partial^4 w_s}{\partial x^2\partial t^2}) \quad (11)$$

Eqs. (9)–(11) are derived using Hamilton's principle, following a procedure similar to that presented by Barati *et al.* [17]. However, the present work incorporates the effects of varying porosity distribution.

The above equations I_i is the mass inertia; k_i *(i=L, P, NL)* is the foundation parameter; N_x is membrane force; M^b and M^s specify the membrane moments which are found based on the theory of nonlocal. The nanobeam rests on a nonlinear elastic foundation, which is modeled using a combination of Winkler, Pasternak, and nonlinear springs. The foundation's reaction force per unit length (q) can be expressed as: $q=k_Lw+k_p\frac{\partial^2 w}{\partial v^2}+k_{NL}w^3$, where: k_L is the Winkler foundation coefficient, representing the stiffness of a distributed array of linear springs. This term accounts for the vertical support provided by the foundation. Units: N/m². k_p is the Pasternak foundation coefficient, representing the shear stiffness of the

foundation. This term accounts for the interaction between the Winkler springs and adds a shear layer to the foundation model. Units: N. k_{NL} is the nonlinear foundation coefficient. This term introduces a cubic nonlinearity to represent the hardening or softening behavior of the foundation under large deflections. Units: N/m⁴. The differences between these coefficients are crucial for accurately capturing the foundation's mechanical behavior. The Winkler coefficient provides only vertical support, while the Pasternak coefficient accounts for shear interactions within the foundation. The nonlinear coefficient allows for modeling the changes in foundation stiffness with increasing deflection. Depending on the specific foundation material and configuration, the relative importance of each coefficient will vary.

$$N_x = A[\frac{\partial u}{\partial x} + \frac{1}{2}(\frac{\partial w}{\partial x})^2] \tag{12}$$

$$\begin{aligned} M_x^b = &-D\frac{\partial^2 w_b}{\partial x^2} - E\frac{\partial^2 w_s}{\partial x^2} + (ea)^2(-N_x\frac{\partial^2(w_b+w_s)}{\partial x^2} + k_L(w_b+w_s) - k_P\frac{\partial^2(w_b+w_s)}{\partial x^2} \\ &+k_{NL}(w_b+w_s)^3 + I_0\frac{\partial^2(w_b+w_s)}{\partial t^2} - I_2(\frac{\partial^4 w_b}{\partial x^2\partial t^2}) - I_4(\frac{\partial^4 w_s}{\partial x^2\partial t^2})) \end{aligned} \tag{13}$$

$$\begin{aligned} M_x^s = &-E\frac{\partial^2 w_b}{\partial x^2} - F\frac{\partial^2 w_s}{\partial x^2} + (ea)^2(-N_x\frac{\partial^2(w_b+w_s)}{\partial x^2} - \frac{\partial Q_{xz}}{\partial x} + k_L(w_b+w_s) - k_P\frac{\partial^2(w_b+w_s)}{\partial x^2} \\ &+k_{NL}(w_b+w_s)^3 + I_0\frac{\partial^2(w_b+w_s)}{\partial t^2} - I_4(\frac{\partial^4 w_b}{\partial x^2\partial t^2}) - I_5(\frac{\partial^4 w_s}{\partial x^2\partial t^2})) \end{aligned} \tag{14}$$

$$(1-(ea)^2\nabla^2)Q_{xz} = A_s\frac{\partial w_s}{\partial x} \tag{15}$$

where *ea* is termed nonlocal coefficient and:

$$\begin{aligned} &A = \int_{-h/2}^{h/2} E(z)\,dz,\ D = \int_{-h/2}^{h/2} E(z)(z-z^*)^2\,dz,\ E = \int_{-h/2}^{h/2} E(z)(z-z^*)(f-z^{**})\,dz \\ &F = \int_{-h/2}^{h/2} E(z)(f-z^{**})^2\,dz,\quad A_s = \int_{-h/2}^{h/2}\frac{E(z)}{2(1+v)}g^2 dz \end{aligned} \tag{16}$$

By including the overwritten equations as Eqs. Additionally, the authors can receive the governing equation of the nanobeam following a specific mathematical procedure that is evident in earlier studies:

So, these are two equations that are not local, and thus they cannot be solved by a standard method.

$$\begin{aligned} &-D(\frac{\partial^4 w_b}{\partial x^4}) - E(\frac{\partial^4 w_s}{\partial x^4}) + A(+\frac{1}{2L}\int_0^L(\frac{\partial w}{\partial x})^2 dx)\frac{\partial^2 w}{\partial x^2} - \mu A(+\frac{1}{2L}\int_0^L(\frac{\partial w}{\partial x})^2 dx)\frac{\partial^4 w}{\partial x^4} \\ &+(1-\mu\frac{\partial^2}{\partial x^2})(-I_0\frac{\partial^2(w_b+w_s)}{\partial t^2} + I_2(\frac{\partial^4 w_b}{\partial x^2\partial t^2}) + I_4(\frac{\partial^4 w_s}{\partial x^2\partial t^2}) - k_L(w_b+w_s) \\ &+k_P\frac{\partial^2(w_b+w_s)}{\partial x^2} - k_{NL}(w_b+w_s)^3) = 0 \end{aligned} \tag{17}$$

$$\begin{aligned} &-E(\frac{\partial^4 w_b}{\partial x^4}) - F(\frac{\partial^4 w_s}{\partial x^4}) + A(+\frac{1}{2L}\int_0^L(\frac{\partial w}{\partial x})^2 dx)\frac{\partial^2 w}{\partial x^2} - \mu A(+\frac{1}{2L}\int_0^L(\frac{\partial w}{\partial x})^2 dx)\frac{\partial^4 w}{\partial x^4} \\ &+(1-\mu\frac{\partial^2}{\partial x^2})(-I_0\frac{\partial^2(w_b+w_s)}{\partial t^2} + I_4(\frac{\partial^4 w_b}{\partial x^2\partial t^2}) + I_5(\frac{\partial^4 w_s}{\partial x^2\partial t^2}) + A_s(\frac{\partial^2 w_s}{\partial x^2}) - k_L(w_b+w_s) \\ &+k_P\frac{\partial^2(w_b+w_s)}{\partial x^2} - k_{NL}(w_b+w_s)^3) = 0 \end{aligned} \tag{18}$$

B. Geometric Nonlinearity

The present study incorporates von Kármán type geometric nonlinearity to account for the large deflections of the nanobeam. This type of nonlinearity considers the nonlinear strain-displacement relations arising from moderate rotations while neglecting in-plane displacements. This is a common approach for modeling beams and plates undergoing relatively large deflections.

C. Derivation of Governing Equations

The nonlinear governing equations are derived using Hamilton's principle, which states that the variation of the total energy of the system must be zero:

$$\delta \int_{t1}^{t2} (T - U + W) dt = 0 \tag{19}$$

where T is the kinetic energy, U is the strain energy, and W is the work done by external forces and the foundation.

(1) Kinetic Energy (T): The kinetic energy is derived considering both translational and rotational inertia terms based on the displacement field, including the second-order shear deformation theory assumptions.

(2) Strain Energy (U): The strain energy is formulated using the von Kármán nonlinear strain-displacement relationships, which include the nonlinear terms arising from the mid-plane stretching due to large deflections. The constitutive relations for the porous material are then used to express the strain energy in terms of the displacements.

(3) Work Done (W): This term accounts for the work done by the nonlinear elastic foundation, including the linear and nonlinear Winkler-Pasternak foundation parameters.

(4) Applying Hamilton's principle and integrating by parts leads to the coupled nonlinear partial differential equations governing the transverse and axial displacements of the nanobeam. These equations include terms related to the nonlocal effect, porosity, and geometric nonlinearity.

III. Method of Solution

The authors have, in this study, embraced the closed-form solution achieved by other research teams [17]. Before doing so, it is essential to describe the placements:

$$w_b = \sum_{m=1}^{\infty} W_{bm}(t) X_m(x) \tag{20}$$

$$w_s = \sum_{m=1}^{\infty} W_{sm}(t) X_m(x) \tag{21}$$

where W_{bmn} and W_{smn} are maximum amplitudes, and the functions X_m could be defined as:

S-S edges

$$\mathrm{X}_m(x) = \sin(\lambda_m x), \quad \lambda_m = \frac{m\pi}{a} \tag{22}$$

C-C edges

$$\mathrm{X}_m(x) = \sin(\lambda_m x) - \sinh(\lambda_m x) - \xi_m(\cos(\lambda_m x) - \cosh(\lambda_m x)), \quad \xi_m = \frac{\sin(\lambda_m x) - \sinh(\lambda_m x)}{\cos(\lambda_m x) - \cosh(\lambda_m x)}, \quad \lambda_1 = 4.730 \tag{23}$$

As a result, the closed-form description of the non-linear frequency of vibration could be written:

$$\omega_{NL} = \sqrt{\frac{1}{2S_1}\left\{(S_2 + S_3) - [(S_2 + S_3)^2 - 4S_1(S_4 + S_5)]^{\frac{1}{2}}\right\}} \tag{24}$$

So in such a way that

$$\begin{aligned} S_1 &= m_{1,1}m_{2,2} - m_{1,2}^2, \Lambda_2 = k_{1,1}m_{2,2} + k_{2,2}m_{1,1} - 2k_{1,2}m_{1,2}, \\ S_3 &= \frac{3}{4} W^{*2} k_{1,3}(m_{1,1} + m_{2,2} - 2m_{1,2}), \\ S_4 &= k_{1,1}k_{2,2} - k_{1,2}^2, \\ S_5 &= \frac{3}{4} W^{*2} k_{1,3}(k_{1,1} + k_{2,2} - 2k_{1,2}), \end{aligned} \tag{25}$$

The maximum deflections are returned by W^* and

$$k_{1,1} = -D\Upsilon_{40} - K_L(\Upsilon_{00} - \mu_0\Upsilon_{20}) + K_P(\Upsilon_{20} - \mu_0\Upsilon_{40}) \tag{26}$$

$$k_{1,1} = -D\Upsilon_{40} - K_L(\Upsilon_{00} - \mu_0\Upsilon_{20}) + K_P(\Upsilon_{20} - \mu_0\Upsilon_{40}) \tag{26a}$$

$$k_{1,2} = k_{2,1} = -E\Upsilon_{40} - K_L(\Upsilon_{00} - \mu_0\Upsilon_{20}) + K_P(\Upsilon_{20} - \mu_0\Upsilon_{40}) \tag{26b}$$

$$k_{2,2} = -F\Upsilon_{40} - K_L(\Upsilon_{00} - \mu_0\Upsilon_{20}) + K_P(\Upsilon_{20} - \mu_0\Upsilon_{40}) + A_s\Upsilon_{20} \tag{26c}$$

$$G^* = A(\frac{1}{2L}\Upsilon_{11}\Upsilon_{20}) - \mu A(\frac{1}{2L}\Upsilon_{11}\Upsilon_{40}) - K_{NL}(\Upsilon_{0000} - \mu_0(6\Upsilon_{1100} + 3\Upsilon_{2000})) \tag{26d}$$

$$m_{1,1} = +I_0\Upsilon_{00} - \mu I_0\Upsilon_{20} - I_2\Upsilon_{20} + \mu I_2\Upsilon_{40} \tag{26e}$$

$$m_{1,2} = m_{2,1} = +I_0\Upsilon_{00} - \mu I_0\Upsilon_{20} - I_4\Upsilon_{20} + \mu I_4\Upsilon_{40} \tag{26f}$$

$$m_{2,2} = +I_0\Upsilon_{00} - \mu I_0\Upsilon_{20} - I_5\Upsilon_{20} + \mu I_5\Upsilon_{40} \tag{26g}$$

where:

$$\{\Upsilon_{00}, \Upsilon_{20}, \Upsilon_{40}, \Upsilon_{11}\} = \int_0^L \{X_m X_m, X_m'' X_m, X_m'''' X_m, X_m' X_m'\} dx$$

$$\{\Upsilon_{0000}, \Upsilon_{1100}, \Upsilon_{2000}\} = \int_0^L \{X_m X_m X_m X_m, X_m' X_m' X_m X_m, X_m'' X_m X_m X_m\} dx$$

These calculations could be derived from the resulting standardized metrics:

$$\hat{\omega} = \omega L^2 \sqrt{\frac{\rho_2 A}{E_2 I}},\ K_L = k_L \frac{L^4}{D},\ K_p = k_p \frac{L^2}{D},\ K_{NL} = k_{NL} \frac{L^4}{A},\ \mu = \frac{e_0 a}{L} \tag{27}$$

IV. Results and Discussions

After deriving the nonlinear vibration frequency of the closed metal nanobeam depicted in Fig. 1, we can analyze its dependence on various factors, including the number and distribution of pores, elastic support, geometric properties, and nonlocal effects. For this analysis, the material properties are set as follows: Young's modulus (E = 200 GPa), density = 7850 kg/m^3, and Poisson's ratio (v = 0.33). Table II presents the frequency verification, which illustrates the accuracy of the adopted method.

TABLE II. Verification of Normalized Frequency Due to Numerous Nonlocal Parameters

No.	Salari and Ebrahimi article	This work
0	9.8594	9.8567
1	9.4062	9.4036
2	9.0102	9.0077
3	8.6603	8.6579

In Fig. 2, we observe how the nonlinear frequency of the nanobeam varies with the nonlocal coefficient and the cavity coefficient for a length (L = 10 h). The distribution of voids or pores is uniform across different coefficient values. The oscillation frequency of the beam can be set by selecting a nonlocal parameter of zero. The figure shows that the nonlocal term, when combined with a low vibration frequency, has a stiff compensation effect. Additionally, an increase in the void fraction decreases the frequency, regardless of the value of the nonlocal parameter.

The nonlocal parameter, which accounts for small-scale effects, is considered within the 0 to 2 nanometers range. This range is consistent with values reported in experimental and theoretical studies on similar nanoscale structures, such as carbon nanotubes and graphene sheets. The value of nonlocal parameter = 0 corresponds to classical local elasticity theory, which ignores size effects. In contrast, higher values of nonlocal parameter indicate increasing nonlocal effects. By selecting a within this range, we can investigate how nonlocal effects influence the nonlinear vibration characteristics and examine how these behaviours deviate from classical prediction

A. Nonlocal Parameters and Real-World Applications

The selected range of nonlocal parameter values (0–2 nm) is especially relevant for various real-world applications:

1. Carbon Nanotube-Based Resonators and Sensors: Carbon nanotubes, commonly used in Nanoscale Electromechanical Systems (NEMS), exhibit nonlocal behavior within this range. Utilizing a nonlocal model enables us to accurately predict these devices' resonant frequencies and sensitivity.

2. Graphene-Based Nano-Devices: Like carbon nanotubes, graphene demonstrates size-dependent mechanical behavior. The chosen nonlocal parameter values can be used to model its dynamic response in numerous applications, such as nano-switches and transistors.

3. Polymer-Based Nanocomposites: The nonlocal theory can also be applied to examine the behavior of polymer nanocomposites reinforced with nanomaterials like graphene or carbon nanotubes. In these cases, the interfacial interactions between the matrix and the reinforcement can introduce nonlocal effects.

Focusing on this range of nonlocal parameters, our study offers valuable insights into the design and optimization of nanoscale devices, where accurately predicting vibrational characteristics is crucial for performance and reliability. Understanding the shifts in resonant frequencies due to nonlocal effects is essential for avoiding undesirable resonances or for designing devices to operate at specific frequencies.

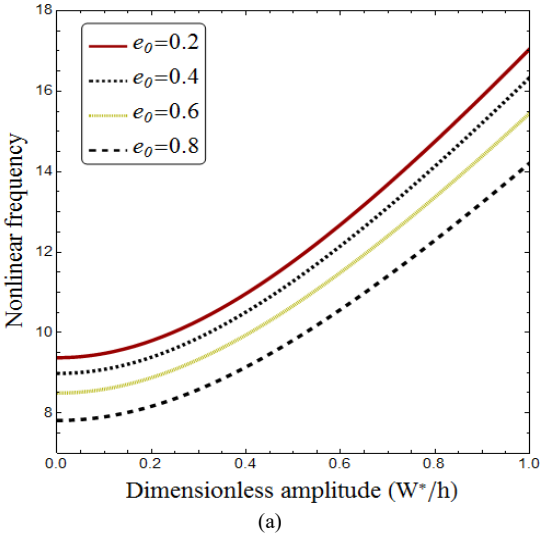

(a)

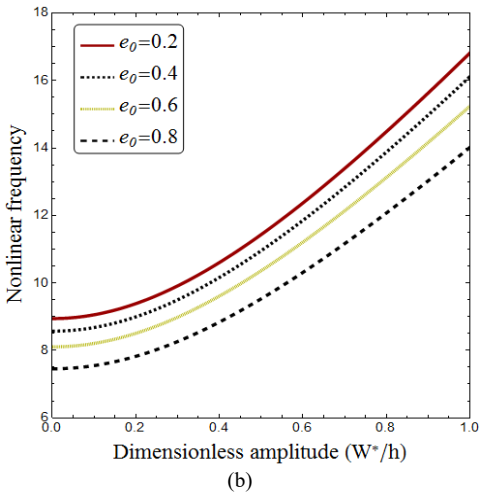

(b)

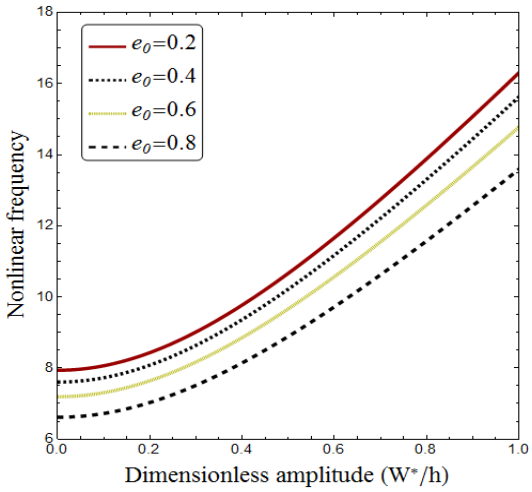

(c)

Fig. 2. The frequency at which the normal mode is expressed as a percentage of the maximum deflection for different values of the void coefficient and nonlocal parameters (L/h = 10): (a) μ = 0; (b) μ = 0.1; (c) μ = 0.2.

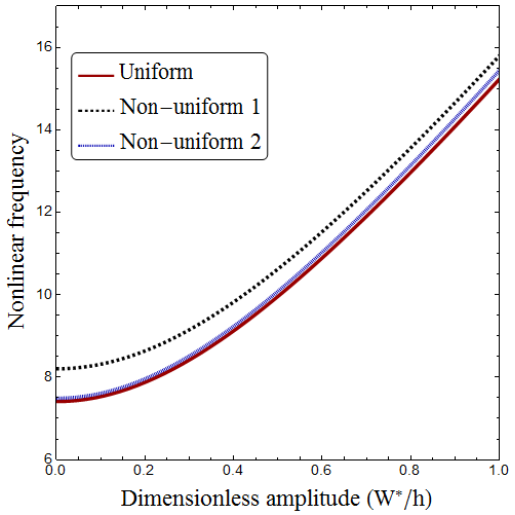

(a)

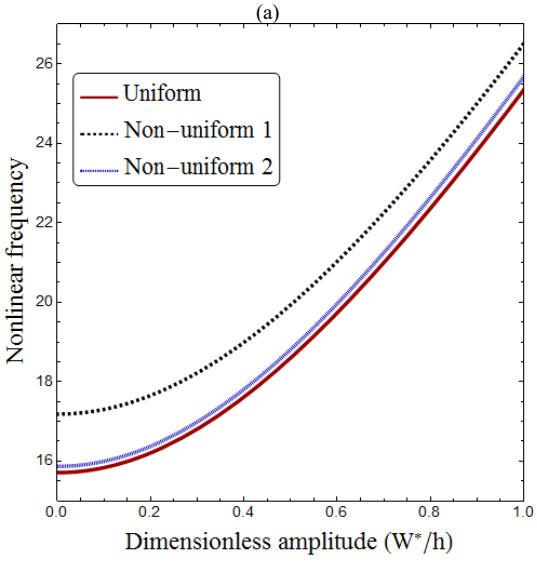

(b)

Fig. 3. The frequency at which the normalised power is equal to the maximum potential for different types of voids (L/h = 10, K_L = 0, K_p = 0, μ = 0.2): (a) S-S; (b) C-C.

Fig. 3 shows the variation in the nonlinear frequency of supported (S-S) and clamped-clamped (C-C) nanobeams based on the type of porosity, with a nonlocal coefficient of $\mu = 0.2$. The data indicates that nanobeams with a single pore type exhibit the highest vibration frequency, followed closely by those with uniform and two pore types. This behavior suggests that nanobeams with identical porous structures possess the greatest stiffness and exhibit the most advantageous properties.

Fig. 4 illustrates the change in nonlinear frequency concerning the slenderness ratio (L/h) for different pore types…It is essential to recognize that a higher slenderness ratio corresponds to a longer and thinner beam with a lower bending rigidity. However, the nonlinear frequency shown in Fig. 4 exhibits an increasing trend with the slenderness ratio. This can be explained by the expanding influence of geometric nonlinearity as the beam becomes slenderer. Slender beams are more susceptible to large deflections, which amplifies the nonlinear effects and consequently leads to a higher nonlinear frequency.

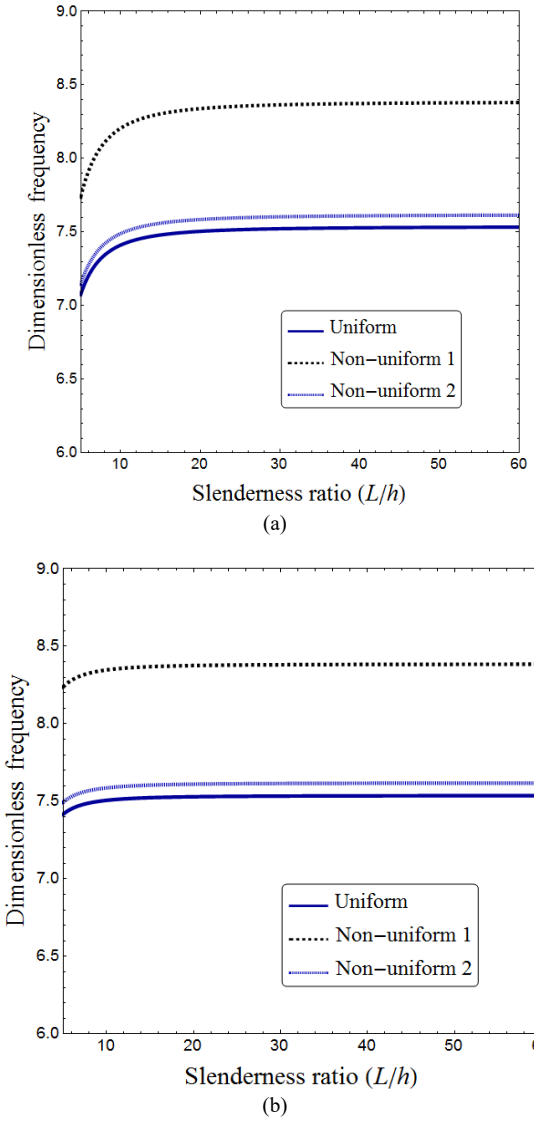

Fig. 4. Normalized non-linear frequency versus slenderness ratio for various void distributions ($K_L = 0$, $K_p = 0$, $\mu = 0.2$, $e_0 = 0.5$): (a) Higher order refined; (b) CBT.

Fig. 5 depicts the variation in nonlinear frequency concerning the maximum deflection at L/h = 10 influenced by the foundation parameters. The key takeaway is the dependence of the nonlinear base coefficient (KNL) on the maximum displacement of the nanobeam. Furthermore, while all foundation parameters increase the nonlinear frequency, it is noteworthy that the linear and shear parameters do not correlate with the maximum displacement.

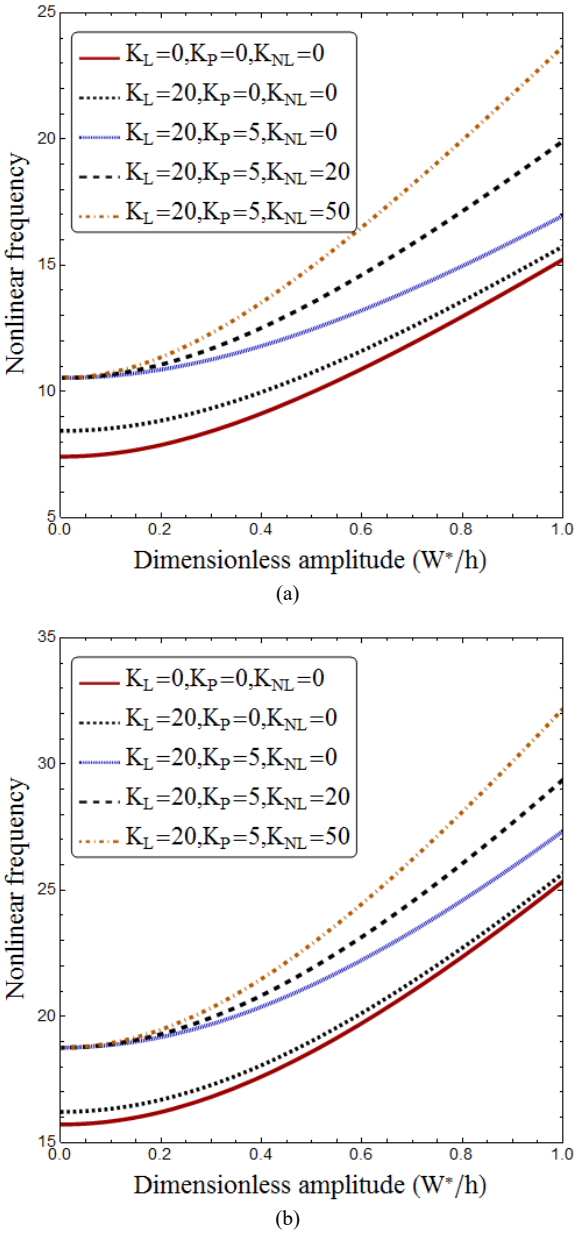

Fig. 5. Normalized frequency of non-linear plotted against Max. deflection for various foundation of L/h = 10, $\mu = 0.2$, $e_0 = 0.5$: (a) S-S; (b) C-C.

Modal Analysis Approach: Our method begins with the assumption that only a finite number of mode shapes of deformation are needed to represent the behaviour of nanobeams adequately, with simple clamped boundary cases only, to implement a closed form. This work does not fully take into account complex higher modes, which require time-consuming finite element simulations to

generate system matrices. Eringen Nonlocal Elasticity: The Eringen nonlocal model helps incorporate size dependence, but it has several parameters. One main area is the scale effects based on nonlocal characteristic properties can be effectively determined only by an evaluation using comparisons between prior or current experimental data. Closed-form model assumption: The closed-form expression assumes simplified representations where real material models could involve various nonlinear models of material and porosity. Geometry and Loading Assumptions: The model assumes a nanobeam of simpler geometry that allows closed-form analysis for dynamic features but also calls for additional assumptions or considerations beyond those involved in actual devices, which may also need consideration under static and transient loading cases.

The authors could articulate why the Eringen model is well-suited for this research context. This approach may provide strong justification for adopting a more straightforward, accessible method grounded in a well-established mathematical framework. Moreover, the selection process may hinge on practical feasibility while demonstrating utility across various parametric levels.

(1) Practical computational requirements. While stress-driven approaches and similar formulations can improve modelling accuracy and provide a more accurate representation of material parameters at the micro-nanoscale, they frequently involve additional implementation steps and increased computational costs in many situations. This area remains an active field of research, and numerous design models and theories do not produce closed-form analytical solutions, which our modelling seeks to achieve. Thus, a trade-off between potential errors and the pursuit of high-fidelity calculations may have been a reasonable choice for the specific objectives of this project.

(2) Analytical Insights with Simple Math: The implementation of an Eringen approach illustrates design execution through a set of mathematical tools that enable parametric sensitivities. These sensitivities may not be easily visualized using complex models and numerical evaluations, which are essential when applying recent alternative theories.

(3) Benchmark Data Availability: The body of literature surrounding Eringen has matured to the point of establishing strong connections with previously developed benchmark data for nanomaterial models. Consequently, the application of new methods has been compared to well-established, validated design-based mathematical modelling parameters.

(4) Ease of Access: The tools related to implementation/methodology or available coding frameworks are currently less accessible when considering many complex multivariable approaches in this evolving research area. These approaches require significant implementation and research efforts compared to mature mathematical implementations, such as the current Eringen theory used to develop nanobeam models with straightforward system settings.

(5) Computational Requirements: Previous analyses have highlighted the limitations of complex Finite Element Analysis (FEA) simulations or iterative nonlinear equation solver-based approaches, where computational demands increase significantly. It is important to note that these limitations also apply to recent method-based implementations due to similar issues with nonlinear solver calculations.

B. Influence of Geometry and Material Properties

The observed vibrational behaviour is strongly intertwined with the geometric and material properties of the nanobeams. The slenderness ratio (L/h), as demonstrated in Fig. 4, plays a crucial role. Higher slenderness ratios correspond to thinner beams, which exhibit lower stiffness and consequently lower nonlinear frequencies. This is because thinner beams are more susceptible to bending deformations. Conversely, thicker beams (lower L/h) experience increased shear deformation effects, influencing the nonlinear frequency response as observed in the higher-order shear deformation theory results.

The porosity distribution also significantly impacts the stiffness and, thus, the vibrational behavior. Uniform porosity weakens the structure more evenly, resulting in a lower overall stiffness compared to non-uniform distributions where the solid material is concentrated in specific regions. This explains why nanobeams with a uniform pore distribution exhibit lower frequencies than those with non-uniform porosity (Fig. 3). In the non-uniform cases, the strategic placement of the solid material can offer localized stiffness enhancements. The type of non-uniform distribution (symmetric vs. asymmetric) also plays a role, affecting the bending stiffness and the resulting frequency response due to the difference in material distribution along the beam's thickness.

The void fraction (e_0) directly affects the effective material properties. A higher void fraction means less solid material, reducing the nanobeam's mass and stiffness. While a lower mass might tend to increase the natural frequency, the dominant effect is the reduction in stiffness, leading to a lower overall frequency (Fig. 2). This interplay between mass and stiffness reduction dictates the overall impact of porosity on the vibrational response.

The nonlocal parameter (μ) captures the small-scale effects prominent in nanoscale structures. As the nonlocal effect increases (higher μ), the interaction between atoms becomes more significant, leading to a softening effect in the nanobeam. This softening translates to a decrease in stiffness and, consequently, a lower nonlinear frequency. This effect is observed in Fig. 2, where increasing μ leads to decreased frequency, especially in the lower amplitude regime. At higher amplitudes, the nonlinear effects become more prominent, and the influence of the nonlocal parameter becomes less dominant.

C. Physical Implications

Understanding these relationships is crucial for designing nanobeams for specific applications. For instance, if a high stiffness and high frequency are desired, a lower void fraction and a non-uniform porosity

distribution should be considered. Conversely, a higher void fraction and uniform porosity might be preferable if flexibility is essential. The slenderness ratio should be optimised based on the desired balance between stiffness and weight. The nonlocal parameter must be carefully considered as it significantly influences the dynamic behavior at the nanoscale. By tailoring these parameters, engineers can fine-tune the vibrational characteristics of metal foam nanobeams for applications in Nano-Electromechanical Systems (NEMS), nano-sensors, and other nanoscale devices.

D. Calibration of Nonlocal Parameter

This study examined a range of nonlocal parameters (0–2 nm) based on values reported in the literature for similar nanoscale structures. The exact value of the nonlocal parameter depends on the specific material and geometry. Therefore, calibrating against atomistic simulations or experimental data is necessary for a given nanoplate to achieve accurate and reliable predictions.

Calibration Methods: Several methods can be used to calibrate nonlocal parameter:

1. Molecular Dynamics (MD) Simulations: MD simulations offer insights into atomic-level interactions. They can be employed to determine effective nonlocal parameter by comparing the simulated vibrational frequencies or other mechanical properties with those predicted by the nonlocal continuum model.

2. Experimental Validation: Experimental techniques, such as measuring the resonant frequencies of fabricated nanoplates, can yield valuable data for calibrating the e_a. An appropriate value for the nonlocal parameter can be established by fitting the nonlocal model to the experimental results.

3. Comparison with Higher-Order Theories: We can estimate a value by comparing results obtained from the nonlocal model with those from higher-order continuum theories, which inherently account for some side effects.

V. Conclusions

This paper analyses the nonlinear vibration behaviour of steel nanobeams, considering the foam's properties and the presence of pores. The study reveals that the nonlocal coefficient and a lower vibration frequency are associated with a reduction in stiffness. Furthermore, nanobeams with symmetrical cavity profiles demonstrate the highest stiffness and superior mechanical properties. Additionally, the normalized oscillation frequency is significantly influenced by lower aspect ratios. Another key finding is that the nonlinear foundation coefficient depends on the maximum deflection of the nanobeam.

The authors clearly articulated their novel contribution by incorporating specific approach-based methods into the design of nano-based material systems developed with a higher degree of simplification. This includes the exact added benefits and practical differences compared to some previously published implementations. They also identified explicit gaps and improvements made in this particular aspect.

Conflict of Interest

The authors declare no conflict of interest.

Author Contributions

Ridha A. Ahmed conducted research, analysed the data, and wrote the paper. Wael N. Abdullah was responsible for writing the paper. Raad M. Fenjan analysed the data and enhanced the quality of the paper. Nadhim M. Faleh enhanced the quality of the paper. He also played a key role in the review process, including responding to reviewers and addressing all feedback. Mamoon A. A. Al-Jaafari analysed the data and enhanced the quality of the paper. All authors had approved the final version of the manuscript.

Acknowledgement

The authors would thank Mustansiriyah University (www.uomustansiriyah.edu.iq) Baghdad-Iraq for its assistance in the present work.

References

[1] D. Chen, J. Yang, and S. Kitipornchai, "Elastic buckling and static bending of shear deformable functionally graded porous beam," *Composite Structures*, vol. 133, pp. 54–61, 2015.

[2] A. S. Rezaei and A. R. Saidi, "Application of carrera unified formulation to study the effect of porosity on natural frequencies of thick porous–cellular plates," *Composites Part B: Engineering*, vol. 91, pp. 361–370, 2016.

[3] B. Mechab *et al.*, "Probabilistic analysis of effect of the porosities in functionally graded material nanoplate resting on Winkler–Pasternak elastic foundations," *Applied Mathematical Modelling*, vol. 40, pp. 738–749, 2016.

[4] S. S. Mirjavadi *et al.*, "Transient response of porous FG nanoplates subjected to various pulse loads based on nonlocal stress-strain gradient theory," *European Journal of Mechanics-A/Solids*, vol. 74, pp. 210–220, 2019.

[5] S. S. Mirjavadi *et al.*, "Nonlinear free and forced vibrations of graphene nanoplatelet reinforced microbeams with geometrical imperfection," *Microsystem Technologies*, pp. 1–14, 2019.

[6] N. Wattanasakulpong and V. Ungbhakorn, "Linear and nonlinear vibration analysis of elastically restrained ends FGM beams with porosities," *Aerospace Science and Technology*, vol. 32, no. 1, pp. 111–120, 2014.

[7] S. A. Yahia *et al.*, "Wave propagation in functionally graded plates with porosities using various higher-order shear deformation plate theories," *Structural Engineering and Mechanics*, vol. 53, no. 6, pp. 1143–1165, 2015.

[8] H. A. Atmane *et al.*, "Effect of thickness stretching and porosity on mechanical response of a functionally graded beams resting on elastic foundations," *International Journal of Mechanics and Materials in Design*, pp. 1–14, 2015.

[9] H. A. Atmane *et al.*, "A computational shear displacement model for vibrational analysis of functionally graded beams with porosities," *Steel and Composite Structures*, vol. 19, no. 2, pp. 369–384, 2015.

[10] A. C. Eringen, "On differential equations of nonlocal elasticity and solutions of screw dislocation and surface waves," *Journal of Applied Physics*, vol. 54, pp. 4703–4710, 1983.

[11] S. Natarajan *et al.*, "Size-dependent free flexural vibration behavior of functionally graded nanoplates," *Computational Materials Science*, vol. 65, pp. 74–80, 2012.

[12] I. Belkorissat *et al.*, "On vibration properties of functionally graded nano-plate using a new nonlocal refined four variable model," *Steel and Composite Structures*, vol. 18, no. 4, pp. 1063–1081, 2015.

[13] R. A. Ahmed, R. M. Fenjan, and N. M. Faleh, "Analyzing post-buckling behavior of continuously graded FG nanobeams with geometrical imperfections," *Geomechanics and Engineering*, vol. 17, pp. 175–180, 2019. doi: 10.12989/gae.2019.17.2.175

[14] A. F. Al-Maliki, N. M. Faleh, and A. A. Alasadi, "Finite element formulation and vibration of nonlocal refined metal foam beams with symmetric and non-symmetric porosities," *Structural Monitoring and Maintenance*, vol. 6, no. 2, pp. 147–159, 2019. doi: 10.12989/smm.2019.6.2.147

[15] M. H. Al-Toki *et al.*, "A numerical study on vibration behavior of fiber-reinforced composite panels in thermal environments," *Structural Engineering and Mechanics*, vol. 82, no. 6, pp. 691–699, 2022. doi: 10.12989/sem.2022.82.6.691

[16] F. Bounouara *et al.*, "A nonlocal zeroth-order shear deformation theory for free vibration of functionally graded nanoscale plates resting on elastic foundation," *Steel and Composite Structures*, vol. 20, no. 2, pp. 227–249, 2016.

[17] M. R. Barati, "Nonlocal-strain gradient forced vibration analysis of metal foam nanoplates with uniform and graded porosities," *Advances in Nano Research*, vol. 5, no. 4, pp. 393–414, 2017.

[18] M. R. Barati, A. M. Zenkour, and H. Shahverdi, "Thermo-mechanical buckling analysis of embedded nanosize FG plates in thermal environments via an inverse cotangential theory," *Composite Structures*, vol. 141, pp. 203–212, 2016.

[19] F. Ebrahimi and M. Daman, "Dynamic modeling of embedded curved nanobeams incorporating surface effects," *Coupled Systems Mechanics*, vol. 5, no. 3, 2016.

[20] F. Ebrahimi and P. Haghi, "A nonlocal strain gradient theory for scale-dependent wave dispersion analysis of rotating nanobeams considering physical field effects," *Coupled Systems Mechanics*, vol. 7, no. 4, pp. 373–393, 2018.

[21] F. Ebrahimi and E. Heidari, "Surface effects on nonlinear vibration and buckling analysis of embedded FG nanoplates via refined HOSDPT in hygrothermal environment considering physical neutral surface position," *Advances in Aircraft and Spacecraft Science*, vol. 5, no. 6, pp. 691–729, 2018.

[22] L. M. Nassir *et al.*, "Transient dynamic analysis of sandwich beam subjected to thermal and pulse load," *Steel and Composite Structures*, vol. 51, no. 1, 2024.

[23] M. A. A. Al-Jaafari *et al.*, "On dynamic deflection analysis of sandwich beams under thermal and pulse loads," *Steel and Composite Structures*, vol. 46, no. 2, 2023.

[24] B. D. Mahdi and N. M. Faleh, "Experimental investigation on segregation process of binary materials based on various vibration conditions," *Asian Journal of Applied Sciences*, vol. 7, no. 4, 2019.

[25] F. Ebrahimi and E. Salari, "Size-dependent free flexural vibrational behavior of functionally graded nanobeams using semi-analytical differential transform method," *Composites Part B: Engineering*, vol. 79, pp. 156–169, 2016.

[26] L. Li, Y. Hu, and L. Ling, "Flexural wave propagation in small-scaled functionally graded beams via a nonlocal strain gradient theory," *Composite Structures*, vol. 133, pp. 1079–1092, 2015.

[27] N. M. Faleh, I. K. Abboud, and A. F. Nori, "Nonlinear stability of smart nonlocal magneto-electro-thermo-elastic beams with geometric imperfection and piezoelectric phase effects," *Smart Structures and Systems*, vol. 25, no. 6, pp. 707–717, 2020. doi: 10.12989/sss.2020.25.6.707

[28] R. M. Fenjan *et al.*, "Nonlocal strain gradient thermal vibration analysis of double-coupled metal foam plate system with uniform and non-uniform porosities," *Coupled Systems Mechanics*, vol. 8, no. 3, pp. 247–257, 2019. doi: 10.12989/csm.2019.8.3.247

[29] H. M. Sedighi *et al.*, "Stress-driven nonlocal elasticity for the instability analysis of fluid-conveying C-BN hybrid-nanotube in a magneto-thermal environment," *Physica Scripta*, vol. 95, no. 6, 2020. doi: 10.1088/1402-4896/ab793f

[30] H. M. Ouakad *et al.*, "On the nonlinear vibration and static deflection problems of actuated hybrid nanotubes based on the stress-driven nonlocal integral elasticity," *Mechanics of Materials*, vol. 48, 2020. doi: 10.1016/j.mechmat.2020.103532

[31] L. Li, Y. Hu, and L. Ling, "Wave propagation in fluid-conveying viscoelastic carbon nanotubes under longitudinal magnetic field with thermal and surface effects via nonlocal strain gradient theory," *Composite Structures*, vol. 153, pp. 992–1003, 2016. doi: 10.1016/j.compstruct.2016.07.014

[32] B. Karami, M. Janghorban, and A. Tounsi, "Galerkin's approach for buckling analysis of functionally graded anisotropic nanoplates/different boundary conditions," *Engineering with Computers*, vol. 35, no. 4, pp. 1297–1316, 2019. doi: 10.1007/s00366-018-0661-z

[33] Y. Zhang, G. Liu, and X. Han, "Thermal buckling of functionally graded porous nanobeams based on nonlocal strain gradient theory," *Composite Structures*, vol. 242, 112150, 2020. doi: 10.1016/j.compstruct.2020.112150

[34] Y. Wang, F. M. Li, and W. H. Huang, "Molecular dynamics study on the mechanical properties of porous graphene nanoplates," *Computational Materials Science*, vol. 186, 110038, 2021. doi: 10.1016/j.commatsci.2020.110038

[35] H. Liu, Y. Zhang, and X. Wang, "Nonlinear vibration analysis of porous functionally graded nanobeams based on nonlocal strain gradient theory and molecular dynamics simulations," *International Journal of Mechanical Sciences*, vol. 214, 106918, 2022. doi: 10.1016/j.ijmecsci.2021.106918

[36] A. Tounsi *et al.*, "A finite element approach for forced dynamical responses of porous FG nanocomposite beams resting on viscoelastic foundations," *International Journal of Structural Stability and Dynamics*, 2650078, 2024.

[37] A. Kadiri *et al.*, "Wave propagation in FG polymer composite nanoplates embedded in variable elastic medium," *Advances in Nano Research*, vol. 17, no. 3, pp. 235–248, 2024. doi: 10.12989/anr.2024.17.3.235

[38] M. Medani *et al.*, "Static and dynamic behavior of (FG-CNT) reinforced porous sandwich plate using energy principle," *Steel and Composite Structures*, vol. 32, no. 5, pp. 595–610, 2019.

[39] B. D. Mahdi and N. M. Faleh, "An experimental investigation on segregation process of binary materials based on various vibration conditions," *Asian Journal of Applied Sciences*, vol. 7, no. 4, 2019. doi: 10.24203/ajas.v7i4.5850

[40] H. Hayyal and N. M. Faleh, "Effect of welding process parameters on tensile of low carbon steel 283 G.C," *Journal of Engineering and Sustainable Development*, vol. 26, no. 1, 2022. doi: 10.31272/jeasd.26.1.8

[41] A. S. Khider *et al.*, "A review on dynamic characteristics of nonlocal porous FG nanobeams under moving loads," *Steel and Composite Structures*, vol. 50, no. 1, pp. 15–24, 2024. doi: 10.12989/scs.2024.50.1.015

[42] B. A. Ghani and N. M. Faleh, "Design study of waste-to-energy system," in *AIP Conference Proceedings*, vol. 2977, 030012, 2023. doi: 10.1063/5.0171234

[43] A. Q. Jbur *et al.*, "Vibration analysis of graphene platelet reinforced stadium architectural roof shells subjected to large deflection," *Structural Engineering and Mechanics*, vol. 86, no. 2, pp. 157–165, 2023. doi: 10.12989/sem.2023.86.2.157

[44] M. A. A. Al-Jaafari *et al.*, "Nonlinear dynamic characteristic of sandwich graphene platelet reinforced plates with square honeycomb core," *Steel and Composite Structures*, vol. 46, no. 5, pp. 659–667, 2023. doi: 10.12989/scs.2023.46.5.659

[45] M. H. Z. Al-Toki *et al.*, "Numerical investigation on dynamic characteristics of sandwich plates under periodic and thermal loads," *Steel and Composite Structures*, vol. 45, no. 6, pp. 831–837, 2022. doi: 10.12989/scs.2022.45.6.831

[46] R. A. Ahmed *et al.*, "A geometrically nonlinear stability analysis of sandwich annular plates with cellular core," *Steel and Composite Structures*, vol. 35, no. 5, pp. 761–774, 2022. doi: 10.12989/scs.2022.35.5.761

[47] M. H. Z. Al-Toki *et al.*, "A numerical study on vibration behavior of fiber-reinforced composite panels in thermal environments," *Structural Engineering and Mechanics*, vol. 82, no. 6, pp. 691–699, 2022. doi: 10.12989/sem.2022.82.6.691

[48] H. A. K. Ali *et al.*, "Nonlinear static analysis of smart beams under transverse loads and thermal-electrical environments," *Advances in Computational Design*, vol. 7, no. 2, pp. 99–112, 2022. doi: 10.12989/acd.2022.7.2.099